

# Magnetic phase transitions in nickel fluosilicate under pressure

V. G. Bar'yakhtar, I. M. Vitebskiĭ, A. A. Galkin, V. P. D'yakonov, I. M. Fita, and G. A. Tsintsadze

*Physicotechnical Institute, Academy of Sciences of the Ukrainian SSR, Donetsk*

(Submitted 29 June 1982)

Zh. Eksp. Teor. Fiz. **84**, 1083–1090 (March 1983)

The magnetic properties of nickel fluosilicate under hydrostatic pressure up to 9.5 kbar have been investigated at temperatures between 0.05 and 0.5 K. The  $P$ - $T$  phase diagram has been constructed. It is shown that the anomalous pressure dependence of the Curie temperature is produced by competition between single-ion anisotropy and exchange interaction.

PACS numbers: 75.30.Kz, 62.50. + p

The present work is devoted to a study of the influence of high hydrostatic pressure on the temperature and nature of the magnetic ordering in nickel fluosilicate.

Fluosilicates form a large group of compounds with the general formula  $MSiF_6 \cdot 6H_2O$ , where  $M$  is a divalent 3d-group cation. Nickel fluosilicate is a double-complex compound  $[Ni(H_2O)_6] \cdot [SiF_6]$  and is described by the Fedorov  $R\bar{3}$  symmetry group.<sup>1</sup> The trigonal axis of the rhombohedral cell and the trigonal axes of the  $Ni(H_2O)_6$  and  $SiF_6$  octahedra coincide with the hexagonal axis of the crystal habit.

The  $NiSiF_6 \cdot 6H_2O$  crystal is one of the model crystals for which the magnetic and resonance properties have been thoroughly studied (the essential references can be found, for example, in Valishev<sup>2</sup>). Ferromagnetic ordering, with magnetic moment parallel to the trigonal axis, is found at atmospheric pressure and temperatures below  $T_C = 0.145$  K.

The ground state of the  $Ni^{2+}$  ion in the crystal field of trigonal symmetry is an orbital singlet with three-fold spin degeneracy ( $S = 1$ ). The spin triplet is split into a singlet and a doublet by the combined action of the trigonal component of the crystal field and spin-orbit interaction. The magnitude of the initial splitting at helium temperatures<sup>1</sup> and atmospheric pressure is  $D = -0.16$  K (the minus sign indicates that the doublet lies below the singlet).

EPR studies of the  $Ni^{2+}$  ions under hydrostatic compression at low temperatures<sup>4</sup> have shown that on increasing the pressure the splitting parameter  $D$  increases and passes through zero at  $P = 1.3$  kbar.

It will be shown below that the specific behavior of  $D$  (which characterizes the single-ion anisotropy) completely determines the topology of the  $P$ - $T$  phase diagram of nickel fluosilicate and also the anomalous pressure dependence of the Curie temperature  $T_C$ .

## EXPERIMENTAL METHOD

The main features of the present experiments is that magnetic measurements were carried out at high hydrostatic pressure (up to 9.5 kbar) at very low temperatures (0.05 to 0.5 K).

A  $^3He$ - $^4He$  dilution refrigerator<sup>5</sup> was used to reach the very low temperatures. The special feature of its design is that the low-temperature part is made as a single module fastened to the thermal flange of the cryostat. A graphite plug separating the evaporation and mixing chambers acts as

a thermal bridge and counter-current heat exchanger. The temperature in the refrigerator was stabilized by a heater and was determined by Speer carbon resistance thermometers calibrated against  $^3He$  vapor pressure (in the range 1.5 to 0.5 K) and by the susceptibility of the paramagnetic salt c.m.n. below 0.5 K. The thermometer resistance was measured by a potentiometric method at direct current. The power dissipated in a thermometer was not more than  $10^{-10}$  W. The estimated error in temperature measurement was  $\pm 5$  mK.

A normal piston and cylinder type of chamber, made of beryllium bronze, was used to produce high hydrostatic pressures. The pressure was determined at helium temperatures from the superconducting transition temperature of a tin single-crystal, and was regulated at room temperature by a manganin gauge. The error in pressure determination was not more than  $\pm 0.1$  kbar.

The high-pressure chamber containing the specimens and measuring coil was immersed directly in the mixing chamber of the refrigerator. Measurements were made on cylindrical single-crystal specimens (diameter 1.5 mm, length 6.0 mm) with axis both parallel and perpendicular to the crystal trigonal axis. An optical method and EPR spectroscopy were used to orient the specimens.

Measurements of the magnetic susceptibility were made with a low-frequency differential magnetometer which differed from that described earlier<sup>6</sup> by having two measuring channels (this allowed the magnetic properties to be studied at a given pressure simultaneously in two crystallographic directions). The amplitude of the alternating magnetic field  $\tilde{h}$  was varied in the range 0.3 to 1.5 Oe and its frequency was 30 Hz. The measuring coil consisted of three pairs of coaxial oppositely wound sections: the specimen was placed in two and a tin single-crystal in the third.

The polarization of the low-frequency field  $\tilde{h}$  (i.e., the direction in which the magnetic susceptibility was measured) coincided in all cases with the cylinder axis  $e$ . The field dependence of the susceptibility  $\chi$  (for various  $P$  and  $T$ ) was also measured with the geometry:

$$\mathbf{h} \parallel \tilde{\mathbf{h}} \parallel \mathbf{e},$$

where  $\mathbf{h}$  is the uniform external magnetic field. A method for continuous recording of the temperature and field dependence of the susceptibility at fixed pressure was used in the experiments.

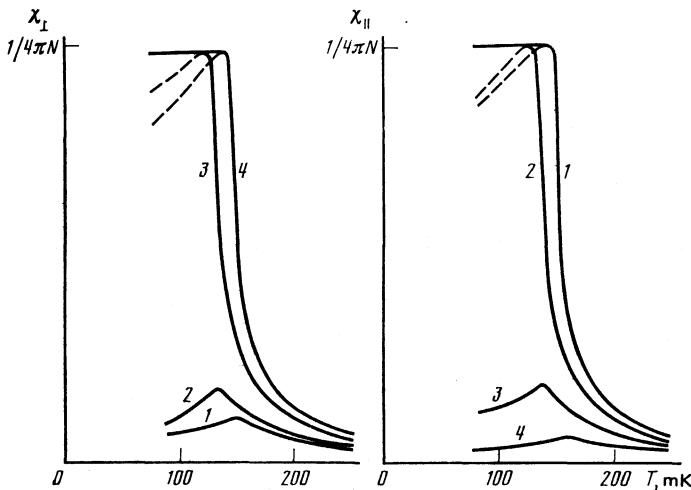


FIG. 1. Temperature dependence of magnetic susceptibility  $\chi_{\parallel}$  and  $\chi_{\perp}$  for fixed pressures and  $\mathbf{h} = 0$ : 1— $P = 0$ , 2— $P = 0.8$ ; 3— $P = 1.9$ ; 4— $P = 3.0$  kbar.

### EXPERIMENTAL RESULTS AND DISCUSSION

Experimental curves of  $\chi(T)$  for  $\mathbf{h} = 0$  are shown in Fig. 1 for several fixed pressures.

On approaching the Curie temperature from the side of the paramagnetic phase, the magnetic susceptibility measured in the easy magnetization direction increases sharply to a value close to  $1/4\pi N$ , where  $N$  is the demagnetizing factor of the specimen. On lowering the temperature further, the susceptibility does not change, indicating the existence of a domain structure. From the fact that at  $P < P_k = 1.3$  kbar this behavior is found only for  $\chi_{\parallel}$  (the susceptibility along the trigonal axis) and at  $P > P_k$  for  $\chi_{\perp}$  (the susceptibility in a direction perpendicular to the trigonal axis), it can be asserted that the magnetization  $\mathbf{m}$  is parallel to the trigonal axis at  $P < P_k$  and that  $\mathbf{m} \perp C_3$  at  $P > P_k$ . There is thus an "easy axis"- "easy plane" magnetic orientational transition induced by pressures at  $P \sim P_k$ .

We note that if the amplitude of the alternating magnetic field on the specimen does not exceed 0.5 Oe, a susceptibility peak is observed at the Curie temperature, while for  $T < T_C$  the susceptibility is appreciably less than the value  $1/4\pi N$ . This is related to the fact that too small an alternating field does not produce a shift of the domain boundaries, so that the susceptibility measured in the easy magnetization direction corresponds to the paramagnetic susceptibility (which is appreciably less than the value of  $1/4\pi N$  for  $T < T_C$ ).

The magnetic  $P$ - $T$  phase diagram of nickel fluosilicate has been constructed (Fig. 2) on the basis of the experimental results. There is no magnetic ordering above the line AKBC (AKBC is the plot of the pressure dependence of the Curie temperature  $T_C$ ). At  $T < T_C$  and  $P < P_k$  there is a ferromagnetic state in which the magnetization is parallel to the crystal trigonal axis, while at  $T > T_C$  and  $P > P_k$  the state has the magnetization vector perpendicular to the  $C_3$  axis. The line KO is the magnetic orientational transition line.

The main features of the phase diagram are the existence of a triple point  $K$ , at which the regions of existence of

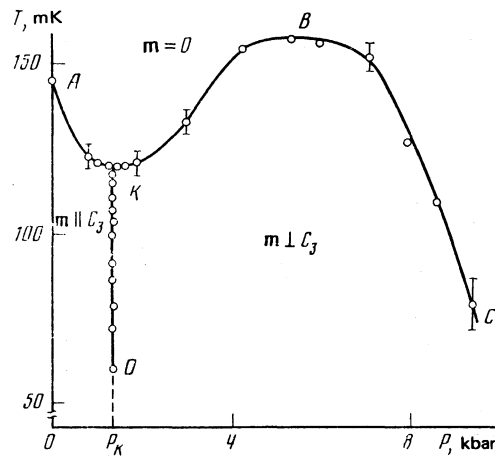


FIG. 2. Magnetic phase diagram for nickel fluosilicate.

the three phases ( $\mathbf{m} = 0$ ;  $\mathbf{m} \parallel C_3$ ;  $\mathbf{m} \perp C_3$ ) meet, and the anomalous behavior of the  $T_C(P)$  dependence. At pressures up to 9.5 kbar the sign of  $dT_C/dP$  changes twice, namely, at the triple point  $K$  and at  $P = 5.8$  kbar.

The spontaneous magnetic moment  $\mathbf{m}$  as a function of  $P$  and  $T$  could be determined from measurements of the magnetic susceptibility in a constant external field  $\mathbf{h}$  parallel to the easy magnetization direction.

The field dependence of the quantity  $\mathbf{M}$ , defined by the relation

$$\mathbf{M}(\mathbf{h}) = \int_0^{\mathbf{h}} \chi(\mathbf{h}) d\mathbf{h}$$

is shown in Fig. 3 for various pressures and temperatures (in all cases  $\mathbf{h} \parallel \mathbf{h} \parallel \mathbf{e}$ ). If it is assumed that the characteristic time for the alternating field  $\tilde{\mathbf{h}}$  to change (of the order of  $1/30$  sec) is, on the one hand, appreciably greater than the spin-spin and spin-lattice relaxation times,<sup>3)</sup> and on the other much less than the thermal relaxation time of the whole specimen relative to the external medium, then the susceptibility measured by us is the adiabatic susceptibility. But the constant field  $\mathbf{h}$  (produced by a superconducting solenoid) is then switched on sufficiently slowly for this process to be considered isothermal.  $\mathbf{M}(\mathbf{h})$  is thus the integral of the adiabatic susceptibility at constant temperature and in general corresponds to neither isothermal nor adiabatic magnetization.

This fact is, however, unimportant in two important particular cases. The connection between the isothermal and adiabatic susceptibilities is actually determined by the thermodynamic relation

$$\chi_{\text{iso}} = \chi_{\text{ad}} + \frac{T}{C_h} \left( \frac{\partial \langle \mathbf{m} \rangle}{\partial T} \right)_h^2,$$

where  $C_h$  is the heat capacity at  $\mathbf{h} = \text{const}$  and  $\langle \mathbf{m} \rangle$  is the magnetization averaged over the domain structure (we denote simply by the letter  $m$  the modulus of the magnetization in each of the ferromagnetic domains). Equality of the isothermal and adiabatic susceptibilities is achieved:

(a) for  $\mathbf{h} = 0$ ; in this case  $\langle \mathbf{m} \rangle = 0$  both in the paraphase and for  $T < T_C$  (because of the existence of the domain structure);

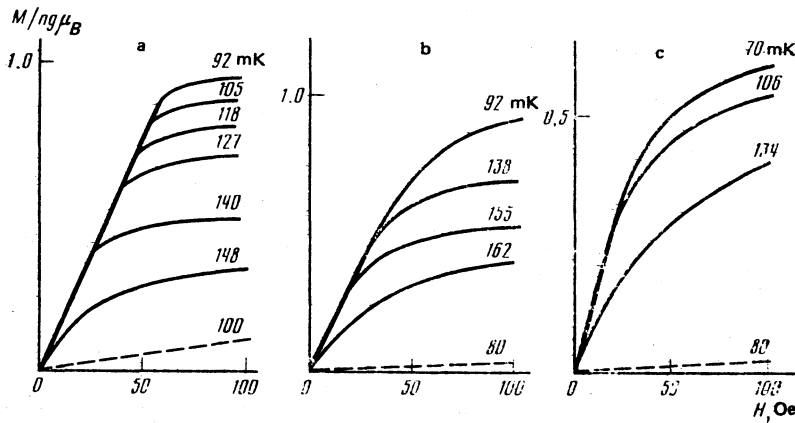


FIG. 3. Variation of  $M(h)$  for various temperatures. The full (dashed) lines refer to the case when  $h$  is parallel (perpendicular) to the direction of easy magnetization: a— $P = 0$  ( $m \parallel C_3$ ); b— $P = 6.0$  ( $m \perp C_3$ ); c— $P = 8.6$  kbar ( $m \perp C_3$ ). The thick full line indicates the straight section of the  $M(h)$  curve with slope  $1/4\pi N$ .

(b) for  $T < T_C$  and  $h < 4\pi Nm$ , when  $h$  is parallel to the easy magnetization axis; in this case  $\langle m \rangle = h/4\pi N$  and is independent of temperature.

The straight line sections of the  $M(h)$  curves in Fig. 3 (with slope  $1/4\pi N$ ) thus correspond simultaneously to both isothermal and adiabatic susceptibilities, while the end of the straight line sections determine the magnitude  $m(T, P)$  of the spontaneous magnetization (in each of the domains).

Experimental curves of the  $m(T)$  dependence obtained in this way for different pressures are shown in Fig. 4.

#### CALCULATION OF THE $P$ - $T$ PHASE DIAGRAM BY THE EFFECTIVE SPIN-HAMILTONIAN METHOD

We use the standard spin Hamiltonian method in the molecular field approximation<sup>4)</sup> for a theoretical interpretation of the experimental results.

The effective Hamiltonian of an individual  $Ni^{2+}$  ion in nickel fluosilicate has the following form:

$$\mathcal{H} = D\hat{S}_z^2 - \mu_B g (H_z \hat{S}_z + H_x \hat{S}_x), \quad (1)$$

where  $\hat{S}$  is the effective  $S = 1$  spin operator; the  $g$ -factor is practically isotropic and equal to 2.24;  $H$  is the effective field equal to the sum of the magnetic field  $h$  and the exchange interaction field  $H^e$ ;

$$H^e = \lambda m = \lambda n \mu_B g \langle \hat{S} \rangle, \quad (2)$$

where  $\lambda$  is the molecular field constant characterizing the isotropic exchange interaction (it has been established that

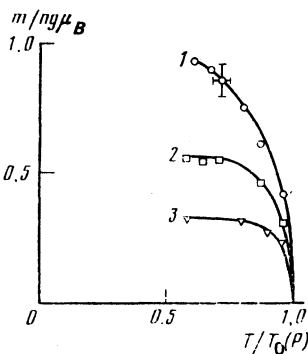


FIG. 4. Temperature dependence of spontaneous magnetization  $m(T)$  for different pressures: 1— $P = 0$  ( $m \parallel C_3$ ); 2— $P = 6.0$  ( $m \perp C_3$ ); 3— $P = 8.6$  kbar ( $m \perp C_3$ ). See Fig. 2 for the  $T_C(P)$  dependence.

the anisotropy and also the biquadratic exchange in  $NiSiF_6 \cdot 6H_2O$  are negligibly small<sup>2)</sup>;  $n$  is the number of magnetic ions in unit volume.

The eigenvalues of the Hamiltonian of Eq. (1) are the roots of the secular equation

$$\epsilon^3 - 2D\epsilon^2 + \epsilon(D^2 - \mu_B^2 g^2 H^2) + D\mu_B^2 g^2 H_x^2 = 0. \quad (3)$$

The magnetization of the crystal is determined by the relation

$$m = -\frac{\partial}{\partial H} (-nT \ln z) = T \frac{n}{z} \frac{\partial z}{\partial H}, \quad (4)$$

where

$$z = \text{Sp} \{ \exp(-\mathcal{H}/T) \} = \sum_{i=1}^3 \exp(-\epsilon_i/T), \quad (5)$$

where  $\epsilon_i$  are the roots of Eq. (3).

The free energy per unit volume of crystal is

$$F = -nT \ln z + 1/2 \lambda m^2. \quad (6)$$

The second term on the right hand side of Eq. (6) is the exchange energy taken with a minus sign (inasmuch as the term  $-nT \ln z$  contains the exchange interaction energy twice).

The magnetic ordering temperature  $T_C$  corresponds to the appearance (for  $T < T_C$ ) of a non-zero solution to Eq. (4) for  $h = 0$ , which corresponds to a minimum in the free energy of Eq. (6). By carrying out the appropriate analysis, we obtain the expressions for  $T_C$ :

$$T_C(2 + e^{D/T_C}) = 3T_0 \quad \text{for } D \leq 0, \quad (7)$$

$$T_C = D \left\{ \ln \frac{3T_0 + 2D}{3T_0 - D} \right\}^{-1} \quad \text{for } D \geq 0, \quad (8)$$

where

$$T_0 = 2/3 \lambda \mu_B^2 g^2 n. \quad (9)$$

The different analytical forms of the expressions for  $T_C$  for  $D < 0$  and  $D > 0$  arise because in the case of  $D < 0$  the minimum in the free energy of Eq. (6) in the magnetically ordered phase corresponds to the state  $m \parallel C_3$ , while in the case of  $D > 0$  it corresponds to  $m \perp C_3$ . In the region of small  $D$  (or more precisely  $|D| \ll T_0$ ) the following approximate expressions for  $T_C$  can be used instead of (7) and (8):

$$T_C \approx T_0 - 1/3 D \quad \text{for } D \leq 0, \quad (10)$$

$$T_C \approx T_0 + 1/6 D \quad \text{for } D \geq 0. \quad (11)$$

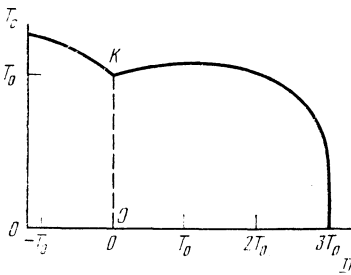


FIG. 5. The dependence of  $T_c$  on  $D$  (in units of  $T_0$ ) according to Eqs. (7) and (8).

The magnetic phase diagram constructed in accordance with (7) and (8) is shown in Fig. 5. The phase diagrams in Figs. (2) and (5) are topologically completely equivalent, but we need to know the  $D(P)$  and  $T_0(P)$  dependences for a quantitative comparison. The corresponding measurements were carried out earlier by the EPR method for the  $\text{Ni}_x\text{Zn}_{1-x}\text{SiF}_6 \cdot 6\text{H}_2\text{O}$  system.<sup>4</sup> According to these studies,  $D$  is a monotonically increasing function of pressure. The  $D(P)$  dependence was in fact determined reliably for any concentrations  $x$  of  $\text{Ni}^{2+}$  ions up to  $x = 1$ . Unfortunately values of  $T_0$  have been measured under pressure reasonably accurately only for  $x \ll 1$  (this is connected with details of the method of measuring EPR spectra). If we, nevertheless, use the  $T_0(P)$  dependence obtained by analyzing the EPR spectrum of exchange-coupled pairs of  $\text{Ni}^{2+}$  ions, then Eq. (8) gives an unlimited increase in  $T_c$  for  $P > P_k$  (we have shown the corresponding curve elsewhere<sup>10</sup>). This sharply contradicts our experiments. It can therefore be assumed that exchange interactions between  $\text{Ni}^{2+}$  ions in  $\text{Ni}_x\text{Zn}_{1-x}\text{SiF}_6 \cdot 6\text{H}_2\text{O}$  for  $x \ll 1$  differ appreciably from those in pure nickel fluosilicate.

Measurement of the paramagnetic susceptibility under pressure is the only reliable means of determining the  $T_0(P)$  dependence in nickel fluosilicate. In fact, by using Eq. (4) it is easy to obtain for  $T \gg D$ ,  $T_0$ <sup>5)</sup>

$$\chi_{zz}^{-1} = c^{-1} \{T - (T_0 - 1/3D)\}, \quad (12)$$

$$\chi_{xx}^{-1} = c^{-1} \{T - (T_0 + 1/6D)\}, \quad (13)$$

where  $c^2 = 2/3 \mu_B^2 g^2 n$ . Thus by knowing the pressure dependence of the paramagnetic Curie temperature

$$\Theta_z = T_0 - 1/3D, \quad \Theta_x = T_0 + 1/6D, \quad (14)$$

the  $T_0(P)$  and  $D(P)$  dependences can be determined directly.

If it turns out that above some pressure  $P^*$  the condition

$$D(P) \geq 3T_0(P) \quad \text{for } P \geq P^*, \quad (15)$$

is satisfied, then according to Eq. (8)

$$T_c = 0 \quad \text{for } P \geq P^*. \quad (16)$$

The inequality which is the inverse of Eq. (15) is in fact the well known Moriya criterion<sup>9</sup> for the occurrence of magnetic ordering in a system of magnetic ions with a singlet ground state (i.e., with  $D > 0$ ). From the experimental  $T_c(P)$  dependence of Fig. 4 it can be expected that the condition of Eq. (15) is satisfied.

Our use of the simplest model based on a Hamiltonian with axial symmetry does not allow us to deal with the question of the nature of the orientational transition between the

states with  $\mathbf{m} \parallel C_3$  and  $\mathbf{m} \perp C_3$  (the line  $KO$  in Figs. 2 and 5). In fact, the magnitude of  $D$  goes to zero for  $P = P_k$  and the Hamiltonian of Eq. (1), and also the free energy therefore, become isotropic (i.e., the direction of the vector  $\mathbf{m}$  is in no way fixed along the phase transition line). It is not difficult, however, to show that this orientational transition for  $P = P_k$  will be a first order transition. To do this we depart from the microscopic model and consider the problem by following a phenomenological method. The expansion of the free energy in powers of the magnetization  $\mathbf{m}$  has the form

$$F = W_{\text{exch}}(m^2) + am_z^2 + bm_z^4 + r_1 m_z(m_+^3 + m_-^3) + ir_2 m_z(m_+^3 - m_-^3), \quad (17)$$

where  $m_{\pm} = m_x \pm im_y$ .

It is easy to show that taking account of the last two terms in Eq. (17) leads to the following effects.

1) The phase transition from the state  $\mathbf{m} \parallel C_3$  to the state  $m_{\perp} \neq 0$  will be a first order transition independently of the magnitude of the constant  $b$ , since these terms are invariants of third order in the corresponding order parameter (the projections  $m_x$  and  $m_y$ ).<sup>6)</sup>

2) The state with  $\mathbf{m} \perp C_3$  is not, strictly speaking, realized; the vector  $\mathbf{m}$  will not lie strictly in the basal plane even for  $P > P_k$ .

We were, unfortunately, unable to observe the existence of these features experimentally. It is possible that this is a result of the smallness of the coefficients  $r_1$  and  $r_2$  in Eq. (17).

<sup>5)</sup>The temperature dependence of  $D$  is solely related to the thermal expansion of the lattice. This effect is negligibly small for  $T < 20$  K.<sup>3</sup>

<sup>6)</sup>A similar effect was observed earlier in the easy ferromagnet  $\text{NiZrF}_6 \cdot 6\text{H}_2\text{O}$ .<sup>7</sup>

<sup>7)</sup>The relaxation time grows without limit in the immediate vicinity of  $T_c$ ,<sup>8</sup> and the assumption stated is invalid.

<sup>8)</sup>The procedure described below is in principle analogous to that used by Moriya<sup>9</sup> in analyzing the magnetic properties of  $\text{NiF}_2$ .

<sup>9)</sup>Accurate measurements of the temperature dependence of  $\chi(T)$  are difficult in this region because of the small magnitude of the magnetic susceptibility. Nevertheless we will carry out the appropriate measurements in the near future.

<sup>10)</sup>A similar effect in a class  $D_{3d}$  rhombohedral ferrite has been studied earlier.<sup>11</sup>

<sup>1)</sup>S. Ray, A. Zalkin, and D. H. Templeton, *Acta Crystallogr.* **B29**, 2741 (1973).

<sup>2)</sup>R. M. Valishev in: *Paramagnitnyĭ rezonans (Paramagnetic Resonance)*, K. G. U. Press, Kazan (1968), p. 35.

<sup>3)</sup>R. P. Penrose and K. W. H. Stevens, *Proc. R. Soc. London Ser. A* **63**, 29 (1950).

<sup>4)</sup>A. A. Galkin, A. Yu. Kozhukhar', and G. A. Tsintsadze, *Zh. Eksp. Teor. Fiz.* **70**, 248 (1976) [*Sov. Phys. JETP* **43**, 128 (1976)].

<sup>5)</sup>A. A. Galkin, V. P. D'yakonov, and I. M. Fita, *Proc. All-Union Conf. on Low Temp. Phys.*, Khar'kov: FTINT Preprint (1980).

<sup>6)</sup>A. A. Galkin, V. P. D'yakonov, I. M. Fita, and G. A. Tsintsadze, *Fiz. Tverd. Tela (Leningrad)* **18**, 3489 (1976) [*Sov. Phys. Solid State* **18**, 2031 (1976)].

<sup>7)</sup>G. V. Lecomte, M. Karnezos, and S. A. Friedberg, *J. Appl. Phys.* **52**, 1935 (1981).

<sup>8)</sup>L. D. Landau and I. M. Khalatnikov, *Dokl. Akad. Nauk SSSR* **96**, 469 (1954).

<sup>9)</sup>T. Moriya, *Phys. Rev.* **117**, 635 (1960).

<sup>10)</sup>A. A. Galkin, I. M. Vitebskii, V. P. D'yakonov, I. M. Fita, and G. A. Tsintsadze, *Pis'ma Zh. Eksp. Teor. Fiz.* **35**, 384 (1982) [*JETP Lett.* **35**, 474 (1982)].

<sup>11)</sup>A. F. Popkov, *Fiz. Tverd. Tela (Leningrad)* **18**, 357 (1976) [*Sov. Phys. Solid State* **18**, 209 (1976)].

Translated by R. Berman